Large-Scale Streamers in the Sedimentation of a Dilute Fiber Suspension

Bloen Metzger,[1] Élisabeth Guazzelli,[1] and Jason E. Butler[2]

[1]*IUSTI - CNRS UMR 6595, Polytech'Marseille, Technopôle de Château-Gombert, 13453 Marseille Cedex 13, France*
[2]*Department of Chemical Engineering, The University of Florida, Gainesville, Florida 32611-6005, USA*

(Received 9 June 2005; published 14 October 2005)

We experimentally characterize structures formed during the sedimentation of rigid fibers of high aspect ratio at small Reynolds number using particle image velocimetry. Measurements show the existence of large-scale streamers during early stages of the sedimentation process, consistent with previously published theory and numerical simulations. At longer times, the cell-wide inhomogeneities evolve into smaller-scale streamers. Measurements of spatially averaged fiber velocities and velocity fluctuations are also presented.

DOI: 10.1103/PhysRevLett.95.164506 PACS numbers: 47.55.Kf, 47.15.Gf, 47.20.−k

Despite being a long-standing problem dating back to the 19th century, the sedimentation of non-Brownian particles at low Reynolds number remains a challenge. The difficulties arise from the long-range nature of the multibody hydrodynamic interactions. The hydrodynamics then depend upon the microstructure of the suspension, i.e., the orientation and relative position of the particles, and the microstructure is in turn determined by the hydrodynamics. This coupling results in a dynamical system which shares features with other problems in nonequilibrium statistical mechanics [1].

The sedimentation rate of a suspension of spheres decreases continuously as the concentration increases [2,3]. Also, theoretical calculations [4] indicate that the suspension is neutrally stable to perturbations in concentration. The sedimentation of rigid fibers differs qualitatively. Theoretical calculations [4] predicted that the coupling between the fiber orientation and flow field generated by the sedimenting fibers leads to a clustering of the particles and subsequent enhancement of the sedimentation rate. The increase of the sedimentation velocity has been observed in particle tracking experiments [5,6] and in simulations using periodic boundary conditions [7–9]; both found that the mean sedimentation rate can exceed the maximum sedimentation rate of an individual particle as given by the sedimentation velocity of a single fiber falling within an unbounded fluid with an orientation parallel to gravity. The simulations determined that the particles tend to orient vertically and cluster into a single streamer which spans the height of the periodic cell. Though Herzhaft *et al.* [5] presented photographs illustrating the formation of concentrated packets containing between 10 and 50 fibers, no quantitative measurement of the inhomogeneous structure in the suspension has been reported.

The present experiments characterize the structures formed by the sedimenting fibers. We show that the dynamics of the flow are dominated by large-scale structures, or streamers, composed of collections of the previously observed clusters [5,6]. The streamers are highly correlated regions of downward velocities induced by relatively local high concentration compared to the mean concentration. To balance the streamers, regions of strong backflow of clarified suspension arise. The occurrence of the large-scale streamer and backflow structures resembles results obtained from simulations in periodic geometries. At later times, the large-scale structures break into smaller streamer and backflow regions. Recent simulations [10], using a point-particle description for a bounded geometry taking into account the presence of walls, found a similar disruption of the streamers as time progressed.

Measurements took place within a glass-walled cell of square cross section ($L_x = L_y = 10$ cm) filled to a height of $L_z = 60$ cm. The sedimentation cell was placed inside a larger tank filled with water to stabilize the sedimenting suspension against the effects of thermal convection. The room temperature was maintained at $23 \pm 1\,^{\circ}$C. The fibers sediment in a Newtonian fluid (25% by volume of UCON oil 75H-90000 and 75% by volume of water) of viscosity $\eta_f = 130 \pm 10$ cP and density $\rho_f = 1.03 \pm .01$ g/cm^3. The nylon fibers were produced by cutting fishing line with a specially designed device. The rigid fibers have an average diameter and length of $d_p = 0.140 \pm .005$ mm and $l_p = 1.52 \pm .05$ mm. The diameter and length measurement are based upon a sample of 430 particles. The aspect ratio is $A = l_p/d_p = 10.8$. The fibers have a density of $\rho_p = 1.13 \pm .02$ g/cm^3.

Based upon the equation of Batchelor [11] (Eq. 2.1 in Herzhaft and Guazzelli [6]), the Stokes velocity of a single, vertical fiber is $V_S = 40 \pm 10\ \mu$m/sec. The error in V_S arises from uncertainties in viscosity, densities, and fiber dimensions. The Reynolds number is $l_p V_S \rho_f/\eta_f \approx 10^{-4}$. All times are scaled by the Stokes time $t_S = 18.9$ sec, the time needed for a fiber with velocity V_S to fall a distance of $l_p/2$, and 10 sec after cessation of mixing is defined as the time of zero. Bending of the fibers and Brownian fluctuations of the fibers are negligible.

A dye added to the particles by the manufacturer of the fishing line fluoresces under illumination provided by a green laser diode. Two such lasers (5 mW power and

 © 2005 The American Physical Society

wavelength of 400–750 nm) positioned on opposite sides of the sedimentation cell were used to create a vertical overlapping laser sheet of thickness 5 mm. The fluorescing fibers are imaged within the plane of the laser sheet using an 8 bit digital camera with a resolution of 1000×1300 pixels and a wide-angle lens. Fluorescing fibers within the laser sheet act as individual light sources and clearly contrast with the other particles in suspension, as seen in Fig. 1.

A series of experiments were carried out on a suspension of volume fraction 0.5%. The suspension was initially mixed thoroughly and the evolution of the structure was observed over a total time of $230t_S$ at intervals of 60 sec. Each observation consists of two images separated in time by 2 sec. Each pair of images was processed using particle image velocimetry (PIV) to find the velocity-vector field. The size of the imaging window was of the width of the cell (10 cm) and 8 cm in height, with the bottom of the imaging window located 15 cm from the bottom of the sedimentation cell. The PIV was performed with an interrogation region, determining the spatial resolution, of 0.53 cm. This spatial resolution is small with regard to the size of the structures, but is large enough to contain a sufficient number of particles to perform PIV and capture the dynamics of the clusters. The measurements were repeated 9 times with the laser sheet located at the center plane of the cell and at a plane offset 2 cm from the center.

Figure 1 compares a raw image of the fluorescing fibers of dimension 3×4 cm at $t = 100t_S$ to the associated velocity field obtained from PIV. The fibers are distributed between regions of relatively high and low concentrations. The regions of high concentration correspond to a high downward velocity, whereas fibers flow upwards within regions of lower density. Direct determination of the distribution of particle concentration is not satisfactory due to the difficulty in characterizing the small concentration differences. Alternatively, the maps of vertical velocity provide a clear measure of the structure dynamics.

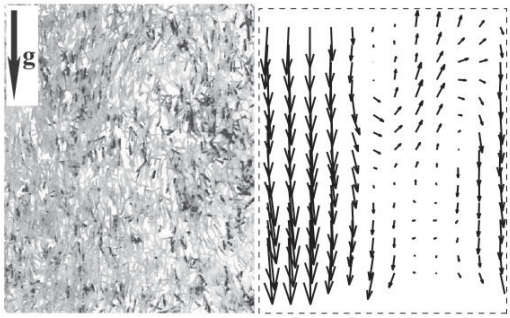

FIG. 1. Image of the fluorescing fibers (in black) within the laser sheet from a subwindow of size 3×4 cm and the corresponding velocity field at a time of $100t_S$. Gravity acts downwards in the images.

Spatiotemporal plots for the magnitude of the vertical velocity were constructed by plotting the vertical velocity profile as a function of time from a horizontal line located 19 cm from the bottom of the cell. Four different experimental runs are shown in Fig. 2. A structure spanning the width of the cell forms during the initial stages of the sedimentation process and the positions of the streamers and backflow persist for long times.

In the early stage of sedimentation ($t < 75t_S$), either a streamer or a region of backflow dominates the center of the viewing window with a seemingly equal probability. Examples of both cases appear in Fig. 2 for the center and off-center planes. The mixing process first resuspends the particles by mixing with an impeller to ensure homogeneity in the height. This is followed by a second stage of mixing by agitating a perforated square plate, which is the same size of the cross section of the cell, up and down within the suspension in order to disrupt the horizontal structure imposed by the impeller mixing. Other mixing processes we attempted substantially biased the location of the large-scale streamers, which is sensitive to the initial conditions since the process is driven by a concentration instability. Simulations [9] have identified a similar sensitivity.

In later stages ($t > 75t_S$), the cell-wide structures passing through the viewing region transition to multiple streamers and backflow regions as shown in Fig. 2. Autocorrelations of the sedimentation velocity fluctuations in the horizontal directions shown in Fig. 3 clarify this evolution. The spatial correlations $C(x)$ in the vertical velocity fluctuations V_z' were computed as $C(x) = \langle V_z'(x_0)V_z'(x_0 + x)\rangle$ ensemble averaged over different starting positions x_0 and the nine runs collected from the center plane. A minimum of $C(x)$, which is negative, indicates an anticorrelation of the vertical velocities along the horizontal direction. At early times, the minimum of the correlation function is

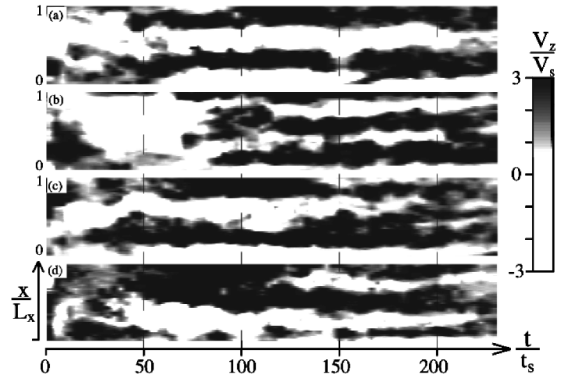

FIG. 2. Vertical velocities as a function of horizontal position and time from two experiments (a) and (b) at a plane offset 2 cm from the center and two experiments (c),(d) at the center plane of the sedimentation cell. Negative velocities (white) represent backflow and positive velocities (black) represent sedimentation.

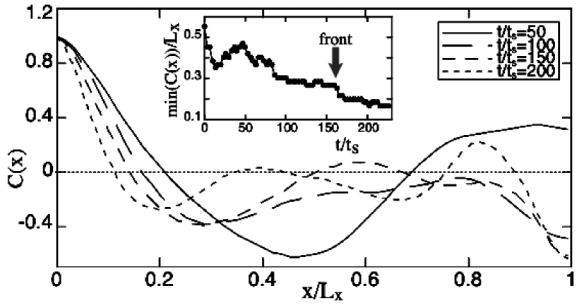

FIG. 3. Autocorrelation of vertical velocity fluctuations in the horizontal direction across the width of the sedimentation cell for data collected from the center-plane images of the viewing window of size 10×8 cm. Inset figure shows the position of the minimum of $C(x)$ as a function of time.

located at $0.5L_x$ in keeping with the qualitative picture of a cell-wide structure of either one streamer in the center or two streamers located near the walls. As time increases, the location of the minimum decreases. Towards the end of the experiment, the minimum moves toward $0.2L_x$ and the correlation pattern indicates an average of 2 or 3 streamers and a corresponding number of 3 or 2 backflow regions.

Structures having half the width of the settling vessel are observed in the early stage of sedimentation. This is consistent with the linear stability theory of Koch and Shaqfeh [4] which predicts that perturbations with the maximum growth rate are those of largest wavelength. Note, however, that Koch and Shaqfeh did not conceive that such wavelength fluctuations would in fact develop. They explain that, for long-wavelength perturbations, the fibers may perform steady rotations in a Jeffery orbit and thus would not induce a growth of the particle density perturbation. They expected perturbations of wavelength $l_p(nl_p^3)^{-1/2}$ to dominate. This is clearly not seen in the experiments as this length scale is of the order of l_p. Simulations with periodic geometry [7–9] also produce a single streamer within the periodic box. Furthermore, the recent simulations with a bottom boundary [10] show a streamer having a size of half the box width in the early stage of sedimentation.

Figure 4 shows that the streamer spans the height of the sedimentation cell. The behavior is reminiscent of results obtained from simulations within periodic geometries [7–9] which produce a single streamer spanning the height of the periodic domains. The breakup of the large-scale streamers observed in the experiments is not captured by the simulations with periodic boundaries, though recent simulations [10] with a bottom boundary do show the breakup of the initial structure into smaller streamers.

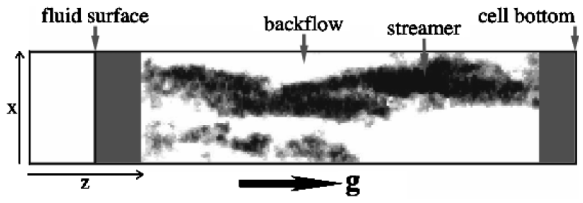

FIG. 4. Vertical velocity at a time of $32t_S$ over the height of the cell. Gravity acts from left to right and the velocity scale is same as in Fig. 2.

The duration of the experiment is limited by the finite height of the experimental vessel. Qualitative measurements of the concentration of the suspension by tracking the intensity of fluorescence as a function of time indicate that the front (as defined by a decrease in intensity to 95% of the initial value) reaches the imaging window at a time of approximately $150t_S$.

Figure 5 shows the mean velocities, $\langle V \rangle$, calculated from all velocity data within the imaging window for the 9 runs from planes located at the center of the cell and 2 cm off center. The error bars on the mean velocities represent the standard deviation of the mean value calculated from each run; note that most of the error arises from calculation of the Stokes velocity which normalizes the mean velocities. The mean velocities in the horizontal direction are on average zero over the duration of the experiment. The mean vertical velocities differ qualitatively depending upon the planar position. For the off-center plane of interrogation, the vertical velocity decreases and reaches a minimum value which is negative at a time of $40t_S$ and then increases in time. The vertical velocity at the center plane increases to a maximum value of $1.5V_S$ at $t = 75t_S$. By $t = 150t_S$, the vertical velocities at the two planes become indistinguishable at a value in excess of V_S within terms of the standard deviation of the means. The velocity fluctuations

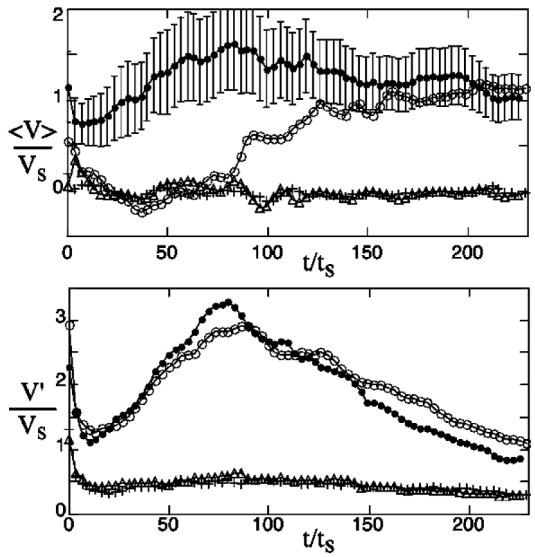

FIG. 5. Mean vertical (circles) and horizontal (triangles) velocities and velocity fluctuations. Results taken from the center plane of the cell (solid symbols) and the plane offset 2 cm from the center (open symbols) are shown. Error bars on the mean velocities represent the standard deviation of the mean values for the different runs.

shown in Fig. 5 are defined as the standard deviation of the velocities as measured over the entire viewing window and number of experimental results. The initial short-time decrease in the velocity fluctuations are due to the quick damping of the mixing process. The velocity fluctuations for both planar positions reach a maximum value of $\approx 3V_S$ at a time of $75t_S$, after which they begin to decline throughout the remainder of the experiment. Note that the probability distribution of the velocities are smooth enough for the mean and variance to represent this distribution.

The difference in mean vertical velocity between the two planes of interrogation for $t < 125t_S$ is due to the random occurrence of stronger backflow regions for some runs at the off-center plane [see Fig. 2(b)] as compared to the center plane. Note that, in this system, the velocity fluctuations are larger than the mean and a large number of runs would be required to sample enough realizations in order to obtain a good estimate of the sedimentation velocity. After $150t_S$, differences in the mean velocities measured at the center and off-center planes diminishes because of the transition to smaller structures and the decrease of the fluctuations. The presence of smaller structures results in a more even distribution of the sampling of streamers and backflow regions across the separate viewing windows. The fluctuations at the center and off-center planes are indistinguishable for all times. They provide information about the velocity differences between streamer and backflow regions.

In previous experiments tracking individual particles within a sampling volume of 1×1 cm and depth of 4 cm in the center of the cell, Herzhaft and Guazzelli [6] found large variations in the mean sedimentation rate which stabilize at a value of $1.5V_S$ for times greater than $50–100t_S$ for a similar aspect ratio and concentration. Large variations of the mean, depending upon the interrogation plane, are also observed in the present experiment for $t < 100t_S$. At the end of the experiments shown in Fig. 5, the mean vertical velocity measured at both planes of interrogation seems also to stabilize and is slightly larger than V_S. Herzhaft and Guazzelli [6] measured large fluctuations in velocity, as seen in the present experiments, but did not examine the variation of the fluctuations with time. Note that Herzhaft and Guazzelli [6] measured local velocities of single particle trajectories, while here we measure spatially averaged velocities (i.e., cluster velocities) only at two planes within the sedimentation cell.

A mean velocity in excess of V_S is also observed in the simulations with periodic boundaries [7–9]. Stabilization is found in those simulations but not in simulations with a bottom bounding wall [10]. This difference has been attributed to the limited height of the cell or to the approximate boundary conditions on the side walls [10]. The same features of a maximum in the velocity fluctuations followed by a decay were observed in simulations with the bottom boundary [10]. In periodic domains, the fluctuations passing through the bottom of the cell are continuously reinjected at the top of the cell, and hence never decay. A similar problem occurs in simulations of sedimenting suspensions of spheres [12,13]. The existence of a bottom prevents this recirculation of the fluctuations, which instead die at the bottom of the sedimentation cell.

In conclusion, we have characterized the evolution of structures during the sedimentation of a dilute suspension of fibers. At the early stage of sedimentation, large-scale streamers, which span the cell width and height, dominate the flow, in agreement with theory and simulations. At longer times, the cell-wide inhomogeneities evolve into smaller-scale structures. During the formation of the large-scale streamers, the fluctuations in the vertical velocity are observed to increase. This is followed by an immediate decrease without observing a steady value. In contrast, the mean vertical velocity remains nearly constant over the time period in which the velocity fluctuations decline. The main result is that particles form clusters which organize into large-scale streamers. The flow evolves from long wavelength—comparable to the cell size—to shorter wavelength. The important remaining question is why the system does not reach a steady behavior in which a saturation of the velocity fluctuations and a wave number selection could be seen.

This study was supported by a collaborative CNRS-NSF research grant. Support from the French Ministère de la Recherche is gratefully acknowledged by B. M. J. E. B. was supported in part by a Chateaubriand grant and by Polytech' Marseille. We thank R. Faure and F. Ratouchniak for technical assistance.

[1] S. Ramaswamy, Adv. Phys. **50**, 297 (2001).
[2] G. K. Batchelor, J. Fluid Mech. **52**, 245 (1972).
[3] R. H. Davis and A. Acrivos, Annu. Rev. Fluid Mech. **17**, 91 (1985).
[4] D. L. Koch and E. S. G. Shaqfeh, J. Fluid Mech. **209**, 521 (1989).
[5] B. Herzhaft, É. Guazzelli, M. B. Mackaplow, and E. S. G. Shaqfeh, Phys. Rev. Lett. **77**, 290 (1996).
[6] B. Herzhaft and É. Guazzelli, J. Fluid Mech. **384**, 133 (1999).
[7] M. B. Mackaplow and E. S. G. Shaqfeh, J. Fluid Mech. **376**, 149 (1998).
[8] J. E. Butler and E. S. G. Shaqfeh, J. Fluid Mech. **468**, 205 (2002).
[9] D. Saintillan, E. Darve, and E. S. G. Shaqfeh, Phys. Fluids **17**, 033301 (2005).
[10] D. Saintillan, E. S. G. Shaqfeh, and E. Darve (to be published).
[11] G. K. Batchelor, J. Fluid Mech. **44**, 419 (1970).
[12] F. R. Da Cunha, Ph.D. thesis, Cambridge University, 1995.
[13] A. J. C. Ladd, Phys. Rev. Lett. **88**, 048301 (2002).